RSC Advances

PAPER

View Article Online
View Journal | View Issue

Cite this: *RSC Adv.*, 2022, **12**, 12878

Luminometric dosimetry of X-ray radiation by a zwitterionic uranium coordination polymer†

Zhaofa Zheng,[bc] Jie Qiu,*[a] Huangjie Lu,[bc] Jian-Qiang Wang *[bc] and Jian Lin *[a]

Received 21st January 2022
Accepted 22nd April 2022

DOI: 10.1039/d2ra00440b

rsc.li/rsc-advances

A novel X-ray dosimeter based on a uranium coordination polymer **U-Cbdcp** was obtained by the judicious synergy between the luminescent uranyl centres and zwitterionic tritopic ligands. Notably, **U-Cbdcp** exhibits luminescence quenching upon increasing X-ray dose, which in combination with its excellent radiolytic stability, makes it suitable for X-ray dosimetry.

X-ray radiation has been extensively used in medical diagnosis and treatment, security screening, quality control inspection, scientific instrumentation, *etc.*[1–3] Overexposure to X-ray radiation cause damage to human cells, which could result in skin burn, tissue damage, and increased incidence of cancer.[4,5] Moreover, X-ray dosimetry is required in many industrial fields, including food irradiation, sterilization, and material modification.[6] Thus, different types of radiation dosimeters, including ionization chamber, scintillator, semiconductor, thermoluminescence dosimeter, chemical dosimeter, and so on, have been commercialized to quantify the incident X-ray dose.[6] The former three types of dosimeters are more frequently applied to record the dose-rate of incident radiation.[7–10] Thermoluminescence dosimeters and chemical dosimeters are suitable for dosimetry of accumulated dose, but they suffer from critical drawbacks such as cumbersome reading processing, instrument-demand, or cost-ineffectiveness.[11,12] Therefore, further development of new types of X-ray dosimeters remains essential.

Coordination polymers, which are assembled from metal ions and organic ligands, have been met with great interest in diverse fields including catalysis, sensing, sorption, separation, and luminescence.[13–18] Their tunability in terms of chemical composition, structure, and more importantly photophysical property, makes them promising for radiation detection. Indeed, pioneering works by Allendorf and co-workers have demonstrated that scintillating metal–organic frameworks (MOFs) assembled from metal cations and radioluminescent organic ligands can function as a new type of radiation detection materials.[13] Furthermore, coordination polymers or cluster species showing radiochromism, radio-photoluminescence, fluorochromism, and photoluminescence quenching upon accumulated doses of ionizing radiation have been documented, making them as promising candidates of radiation dosimeters.[19–26] Notably, the abundance of luminescent centers or radio-responsive moieties in some of these materials renders higher saturation point in response to radiation dose. This attribute allows for wider operation ranges or higher upper limits of detection compared with those of traditional metal-ion-doped inorganic dosimeters, *e.g.* Ag-doped phosphate glass and Mg^{2+}-doped LiF (LiF:Mg).[27]

We have recently undertaken a study focused on developing actinide-based coordination polymers or cluster materials for their promising applications in ionizing radiation detection.[19,21,28] The large coordination numbers and diverse coordination geometries of actinide cations engender a myriad of topologies of these materials.[29–31] Moreover, the intrinsically intense green emission from the uranyl cation can be utilized as a radio-luminescent center.[23,26] In addition, the slight radioactivity of ^{238}U ($t_{1/2}$ = 4.47 billion years) can be neglected in the course of high dose radiation detection.[32,33] Herein, a novel zwitterionic uranium coordination polymer is reported, showing rather unique fluorescence quenching response to X-ray radiation. This radio-responsive feature, in combination with its high radiolytic stability, points to the potential implementation of uranium-bearing materials for radiation dosimetry.

Solvothermal reaction between $UO_2(NO_3)_2 \cdot 6H_2O$, zwitterionic *N*-(4-carboxybenzyl)-(3,5-dicarboxyl)pyridinium bromide (H_3CbdcpBr), and CH_3COOH in DMF/H_2O mixed solution at 100 °C afforded yellow crystals of $UO_2(OH)(H_2Cbdcp)(HCbdcp) \cdot 4H_2O$ (**U-Cbdcp**) with a yield of 63% based on U.

Single crystal X-ray diffraction (SCXRD) analysis revealed that **U-Cbdcp** crystalizes in the monoclinic $P2_1/n$ space group (Table S1†). The asymmetric unit of **U-Cbdcp** network consists of one crystallographically independent UO_2^{2+} cation, two Cbdcp ligands, and one hydroxide group (Fig. S1†). The coordination geometry of uranyl cation can be best described as

[a]*School of Nuclear Science and Technology, Xi'an Jiaotong University, Xi'an, 710049, P. R. China. E-mail: qiujie1228@xjtu.edu.cn; jianlin@xjtu.edu.cn*

[b]*Key Laboratory of Interfacial Physics and Technology, Shanghai Institute of Applied Physics, Chinese Academy of Sciences, 2019 Jia Luo Road, Shanghai 201800, P. R. China. E-mail: wangjianqiang@sinap.ac.cn*

[c]*University of Chinese Academy of Sciences, No. 19(A) Yuquan Road, Shijingshan District, Beijing, 100049, P. R. China*

† Electronic supplementary information (ESI) available: Synthesis, characterizations, PXRD, FTIR, SEM-EDS, crystallographic data, selected bond distances and angles. CCDC 2141552–2141553. For ESI and crystallographic data in CIF or other electronic format see https://doi.org/10.1039/d2ra00440b

a typical pentagonal bipyramid, of which four O atoms on the pentagonal plane are donated from three Cbdcp ligand and the rest one is from a hydroxide group (Fig. 1a).[34–38] One of the organic linkers coordinates with one uranyl cation in a μ_1–η_1 bridging mode, while the other one interconnects with two uranyl cations in a μ_2–η_1:η_2 manner (Fig. 1b). Therefore, these two crystallographically unique ligands can be assigned as H_2-Cbdcp$^-$ and HCbdcp^{2-} with one and two carboxylate group being deprotonated, respectively. The torsion angles between the carboxybenzyl and (3,5-dicarboxyl)pyridinium moieties are measured to be 110.909° and 112.447° for H_2Cbdcp$^-$ and HCbdcp^{2-}, respectively, as defined by ∠N–C–C. The assembly of uranyl cations, H_2Cbdcp$^-$, and HCbdcp^{2-} ligands results in the formation of a one-dimensional infinite chain extending along the *c* axis (Fig. 1c). The afforded chains are further extended into a 3D supramolecular network *via* π–π interactions and hydrogen bonds between the ligands (Fig. 1d). The phase purity of bulky **U-Cbdcp** sample was confirmed by powder X-ray diffraction (PXRD), showing that the measured pattern matches well with the simulated one (Fig. S2†).

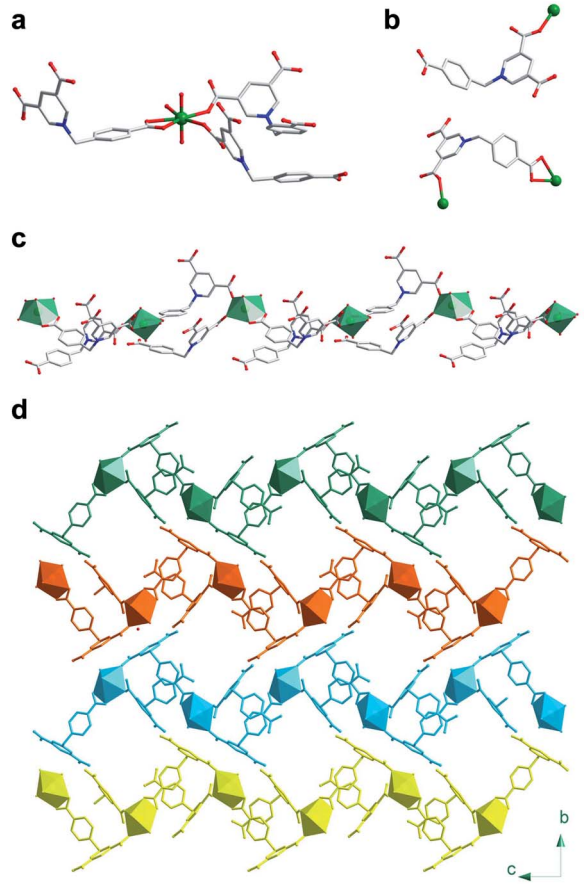

Fig. 1 (a) The coordination environment of UO_2^{2+} cation. (b) The coordination modes of two crystallographically independent ligands. (c) The 1D chain of **U-Cbdcp** extending along the *c* axis. (d) Representation showing the network of **U-Cbdcp**. In figure (a)–(c), U atoms are in green, O atoms are in red, N atoms are in blue, and C atoms are in grey.

The solid-state luminescence spectrum (λ_{ex} = 365 nm) was collected on a tablet of **U-Cbdcp**, that was fabricated from finely ground powder. As expected, **U-Cbdcp** exhibits five characteristic bands of uranyl cation centring at 488, 508, 531, 556, and 583 nm (Fig. 2a). This intense green emission can be attributed to the HOMO-LUMO transition occurring in the uranyl bonds upon UV excitation.[38,39] Strikingly, the uranyl-based luminescence is strongly quenched after X-ray radiation (4.7 kGy) as shown by the photographs of **U-Cbdcp** tablet (Fig. 2a inset). Concomitantly, the intensities of characteristic UO_2^{2+} emission bands, which were measured from the tablet exposed to specific interval of X-ray dose, gradually diminished upon continuous X-ray irradiation (Cu-K$_\alpha$, 120 Gy min^{-1}). More specifically, approximately 44% luminescence intensity was retained after being exposed to 260 Gy X-ray radiation (Fig. 2a). Further increasing the dose to 4.7 kGy resulted in nearly 90% emission quenching. Interestingly, I_0/I as a function of radiation dose can be well fitted with a linear correlation with R^2 of 0.9988, where I_0 and I are the luminescence intensities monitored at 508 nm before and after irradiation, respectively. This excellent linearity allows for quantifying X-ray dose in a wide dynamic range spanning from 10 to 4700 Gy *via* a luminescence "turn-off" manner. To obtain limit of detection (LOD), the calibration curve was established by plotting the quenching rate $(I_0 - I)/I_0$ as a function of dose at the low dose range (0–30 Gy) (Fig. S3†).

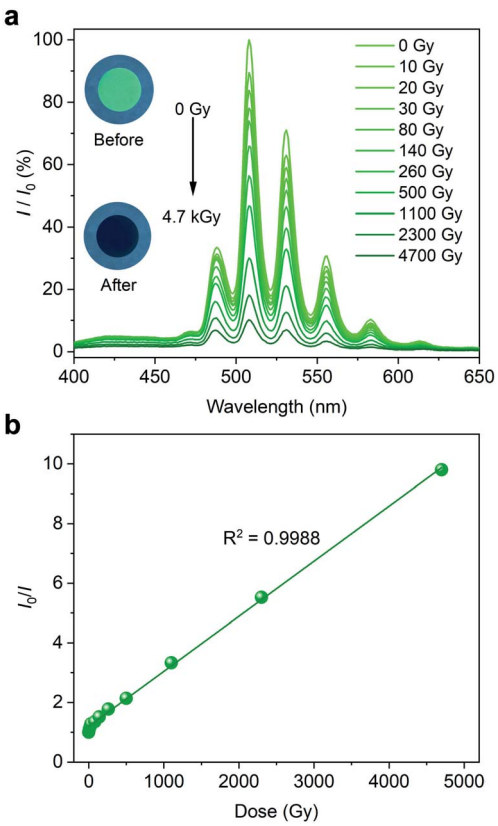

Fig. 2 (a) X-ray dose-dependent fluorescence spectra and optical micrographs (inset) of a **U-Cbdcp** tablet. (b) The plot showing the linear correlation between I_0/I and X-ray dose.

The limit of detection (LOD) is calculated to be 0.093 Gy based on the method reported by Zang and coworkers.[40] Markedly, this LOD is comparable to 0.047 Gy of the most sensitive photochromic sensor Htpbz@Th-SINAP-2.[21]

To decipher the quenching mechanism, the structures of **U-Cbdcp** before and after X-ray irradiation (5 kGy) were thoroughly characterized by combined techniques including PXRD and SCXRD. The PXRD patterns of **U-Cbdcp** remained approximately unchanged upon irradiation, ruling out our initial speculation of radiation induced damage to the bulky sample (Fig. S4†). This supposition is additionally supported by the nearly identical FTIR spectrum of irradiated **U-Cbdcp** with the nonirradiated one (Fig. S5†). Furthermore, SCXRD analysis before and after X-ray radiation was conducted on the same single crystal of **U-Cbdcp** and revealed that the overall network derived from these two datasets retain unchanged as well (Table S1†). In detail, the local structure as represented by the bond length and bond angle of **U-Cbdcp** changes slightly, which can be attributed to the standard deviations of these parameters obtained from SCXRD (Table S2†). This observation further excludes the quenching mechanism *via* decomposition of **U-Cbdcp** crystal.

There is precedence in literature that the luminescence quenching can be associated with the generation of radicals *via* radio-induced bond break or electron transfer.[23,26,41,42] Therefore, electron paramagnetic resonance (EPR) spectrum of irradiated **U-Cbdcp** was collected and indeed shows an intense EPR signal with a *g*-tensor of 2.0197, corresponding to the value (g = 2.0023) of a free electron (Fig. 3).[43] The freshly synthesized sample, however, is EPR silent for comparison. To identify the location of radical species in the coordination polymer, EPR spectra of H_3CbdcpBr ligand before and after irradiation were recorded as well. As shown in Fig. S6,† the irradiated H_3-CbdcpBr exhibits a relatively weak resonance with a *g* factor of 2.0198, which is comparable with that of **U-Cbdcp**. In the light of aforementioned results, we may conclude that continuous X-ray radiation generates ligand-based radical species, which functions as a quencher *via* a nonradiative energy transfer pathway.[44–46]

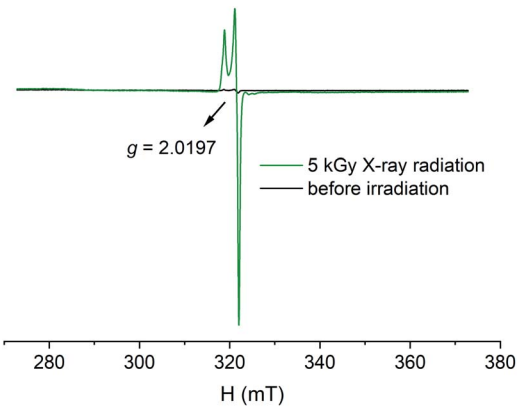

Fig. 3 EPR spectra of **U-Cbdcp** before and after 5 kGy X-ray radiation.

Encouraged by the structural integrity of **U-Cbdcp** upon 5 kGy X-ray irradiation, we further investigated its radiolytic stability by irradiating the sample with high dose β-ray and γ-ray radiations. The radiations were provided by a custom-built electron cyclotron (1.2 MeV) and a ^{60}Co irradiation source (2.22×10^{15} Bq) with dose rates of 150 and 11.8 kGy per h, respectively. PXRD study indicated that no obvious changes in long-range order or loss of crystallinity of **U-Cbdcp** were observed after radiations, implying excellent radiation resistance of **U-Cbdcp** (Fig. S7†).

In summary, a new 1D uranium coordination polymer built from uranyl cations and zwitterionic Cbdcp ligands were obtained solvothermally. One of the most intriguing properties of **U-Cbdcp** is the occurrence of luminescence quenching upon X-ray radiation. This unique radio-induced luminometric response can be utilized as a strategy for X-ray dosimetry. Notably, the quenching response can be well fitted with a linear correlation and the detection limit was calculated to be 0.093 Gy. This finding, in conjunction with the excellent radiation resistance of **U-Cbdcp**, point to potential applications of uranium bearing materials for radiation detection.

Conflicts of interest

The authors declare no competing financial interest.

Acknowledgements

This work was supported by the National Natural Science Foundation of China (22076196, 21876182, 21806127, and U1967219), the Shanghai Sailing Program (21YF1456200) and Natural Science Foundation of Shaanxi Province (2020JM-016).

Notes and references

1 K. Song, M. Mohseni and F. Taghipour, *Water Res.*, 2016, **94**, 341.
2 C. Decker, *Macromol. Rapid Commun.*, 2002, **23**, 1067.
3 P. Suortti and W. Thomlinson, *Phys. Med. Biol.*, 2003, **48**, R1.
4 J. Cadet, E. Sage and T. Douki, *Mutat. Res., Fundam. Mol. Mech. Mutagen.*, 2005, **571**, 3.
5 E. I. Azzam, J. P. Jay-Gerin and D. Pain, *Cancer Lett.*, 2012, **327**, 48.
6 P. Andreo, D. T. Burns, A. E. Nahum, J. Seuntjens and F. H. Attix, *Fundamentals of Ionizing Radiation Dosimetry*, Wiley, 2017.
7 L. Sang, M. Liao and M. Sumiya, *Sensors*, 2013, **13**, 10482.
8 C. Sun, X.-Q. Yu, M.-S. Wang and G.-C. Guo, *Angew. Chem., Int. Ed.*, 2019, **58**, 9475.
9 Y. Wang, X. Liu, X. Li, F. Zhai, S. Yan, N. Liu, Z. Chai, Y. Xu, X. Ouyang and S. Wang, *J. Am. Chem. Soc.*, 2019, **141**, 8030.
10 H. Wei and J. Huang, *Nat. Commun.*, 2019, **10**, 1066.
11 J. Nandha Gopal, B. Sanyal and A. Lakshmanan, *Radiat. Meas.*, 2018, **109**, 24.
12 F. Ravotti, *IEEE Trans. Nucl. Sci.*, 2018, **65**, 1440.
13 F. P. Doty, C. A. Bauer, A. J. Skulan, P. G. Grant and M. D. Allendorf, *Adv. Mater.*, 2009, **21**, 95.

14 S. T. Meek, J. A. Greathouse and M. D. Allendorf, *Adv. Mater.*, 2011, **23**, 249.
15 A. M. Rice, C. R. Martin, V. A. Galitskiy, A. A. Berseneva, G. A. Leith and N. B. Shustova, *Chem. Rev.*, 2020, **120**, 8790.
16 C. R. Martin, G. A. Leith, P. Kittikhunnatham, K. C. Park, O. A. Ejegbavwo, A. Mathur, C. R. Callahan, S. L. Desmond, M. R. Keener, F. Ahmed, S. Pandey, M. D. Smith, S. R. Phillpot, A. B. Greytak and N. B. Shustova, *Angew. Chem., Int. Ed.*, 2021, **60**, 8072.
17 L. Liu, Q. Liu, R. Li, M.-S. Wang and G.-C. Guo, *J. Am. Chem. Soc.*, 2021, **143**, 2232.
18 W.-F. Wang, J. Lu, X.-M. Xu, B.-Y. Li, J. Gao, M.-J. Xie, S.-H. Wang, F.-K. Zheng and G.-C. Guo, *Chem. Eng. J.*, 2022, **430**, 133010.
19 H. Lu, J. Xie, X.-Y. Wang, Y. Wang, Z.-J. Li, K. Diefenbach, Q.-J. Pan, Y. Qian, J.-Q. Wang, S. Wang and J. Lin, *Nat. Commun.*, 2021, **12**, 2798.
20 H. Lu, Z. Zheng, Z.-J. Li, H. Bao, X. Guo, X. Guo, J. Lin, Y. Qian and J.-Q. Wang, *ACS Appl. Mater. Interfaces*, 2021, **13**, 2745.
21 Z. Zheng, H. Lu, X. Guo, Z. Zhou, Y. Wang, Z.-J. Li, G. Xiao, Y. Qian, J. Lin and J.-Q. Wang, *Chem. Commun.*, 2021, **57**, 8131.
22 H. Liu, H. Qin, N. Shen, S. Yan, Y. Wang, X. Yin, X. Chen, C. Zhang, X. Dai, R. Zhou, X. Ouyang, Z. Chai and S. Wang, *Angew. Chem., Int. Ed.*, 2020, **59**, 1.
23 J. Xie, Y. Wang, W. Liu, X. Yin, L. Chen, Y. Zou, J. Diwu, Z. Chai, T. E. Albrecht-Schmitt, G. Liu and S. Wang, *Angew. Chem., Int. Ed.*, 2017, **56**, 7500.
24 X. Li, Y. Wang, J. Xie, X. Yin, M. A. Silver, Y. Cai, H. Zhang, L. Chen, G. Bian, J. Diwu, Z. Chai and S. Wang, *Inorg. Chem.*, 2018, **57**, 8714.
25 W. Liu, X. Dai, J. Xie, M. A. Silver, D. Zhang, Y. Wang, Y. Cai, J. Diwu, J. Wang, R. Zhou, Z. Chai and S. Wang, *ACS Appl. Mater. Interfaces*, 2018, **10**, 4844.
26 J. Xie, Y. Wang, W. Liu, C. Liang, Y. Zhang, L. Chen, D. Sheng, Z. Chai and S. Wang, *Sci. China: Chem.*, 2020, **63**, 1608.
27 F. Nakamura, T. Kato, G. Okada, N. Kawaguchi, K. Fukuda and T. Yanagida, *Ceram. Int.*, 2017, **43**, 7211.
28 H. Lu, M. Xu, Z. Zheng, Q. Liu, J. Qian, Z.-H. Zhang, M.-Y. He, Y. Qian, J.-Q. Wang and J. Lin, *Inorg. Chem.*, 2021, **60**, 18629.
29 E. A. Dolgopolova, A. M. Rice and N. B. Shustova, *Chem. Commun.*, 2018, **54**, 6472.
30 C. R. Martin, G. A. Leith and N. B. Shustova, *Chem. Sci.*, 2021, **12**, 7214.
31 K. Lv, S. Fichter, M. Gu, J. März and M. Schmidt, *Coord. Chem. Rev.*, 2021, **446**, 214011.
32 N. M. Edelstein, J. Fuger and L. R. Morss, *The Chemistry of the Actinide and Transactinide Elements*, Springer, 2010.
33 M. Zhang, C. Liang, G.-D. Cheng, J. Chen, Y. Wang, L. He, L. Cheng, S. Gong, D. Zhang, J. Li, S.-X. Hu, J. Diwu, G. Wu, Y. Wang, Z. Chai and S. Wang, *Angew. Chem., Int. Ed.*, 2021, **60**, 9886.
34 L. Mei, P. Ren, Q.-y. Wu, Y.-b. Ke, J.-s. Geng, K. Liu, X.-q. Xing, Z.-w. Huang, K.-q. Hu, Y.-l. Liu, L.-y. Yuan, G. Mo, Z.-h. Wu, J. K. Gibson, Z.-f. Chai and W.-q. Shi, *J. Am. Chem. Soc.*, 2020, **142**, 16538.
35 G. L. Murphy, Y. Wang, P. Kegler, Y. Wang, S. Wang and E. V. Alekseev, *Chem. Commun.*, 2021, **57**, 496.
36 G. L. Murphy, E. M. Langer, O. Walter, Y. Wang, S. Wang and E. V. Alekseev, *Inorg. Chem.*, 2020, **59**, 7204.
37 H. Li, P. Kegler and E. V. Alekseev, *Dalton Trans.*, 2020, **49**, 2244.
38 X. Kong, K. Hu, L. Mei, Q. Wu, Z. Huang, K. Liu, Z. Chai, C. Nie and W.-Q. Shi, *Chem. - Eur. J.*, 2021, **27**, 2124.
39 M. Azam, S. I. Al-Resayes, G. Velmurugan, P. Venuvanalingam, J. Wagler and E. Kroke, *Dalton Trans.*, 2015, **44**, 568.
40 J.-M. Han, M. Xu, B. Wang, N. Wu, X. Yang, H. Yang, B. J. Salter and L. Zang, *J. Am. Chem. Soc.*, 2014, **136**, 5090.
41 J. Xie, Y. Wang, D. Zhang, C. Liang, W. Liu, Y. Chong, X. Yin, Y. Zhang, D. Gui, L. Chen, W. Tong, Z. Liu, J. Diwu, Z. Chai and S. Wang, *Chem. Commun.*, 2019, **55**, 11715.
42 G. Mehlana and S. A. Bourne, *CrystEngComm*, 2017, **19**, 4238.
43 S. Tang, H. Ruan, R. Feng, Y. Zhao, G. Tan, L. Zhang and X. Wang, *Angew. Chem., Int. Ed.*, 2019, **58**, 18224.
44 T. B. Faust and D. M. D'Alessandro, *RSC Adv.*, 2014, **4**, 17498.
45 B. Lü, Y. Chen, P. Li, B. Wang, K. Müllen and M. Yin, *Nat. Commun.*, 2019, **10**, 767.
46 Y.-J. Ma, J.-X. Hu, S.-D. Han, J. Pan, J.-H. Li and G.-M. Wang, *J. Am. Chem. Soc.*, 2020, **142**, 2682.